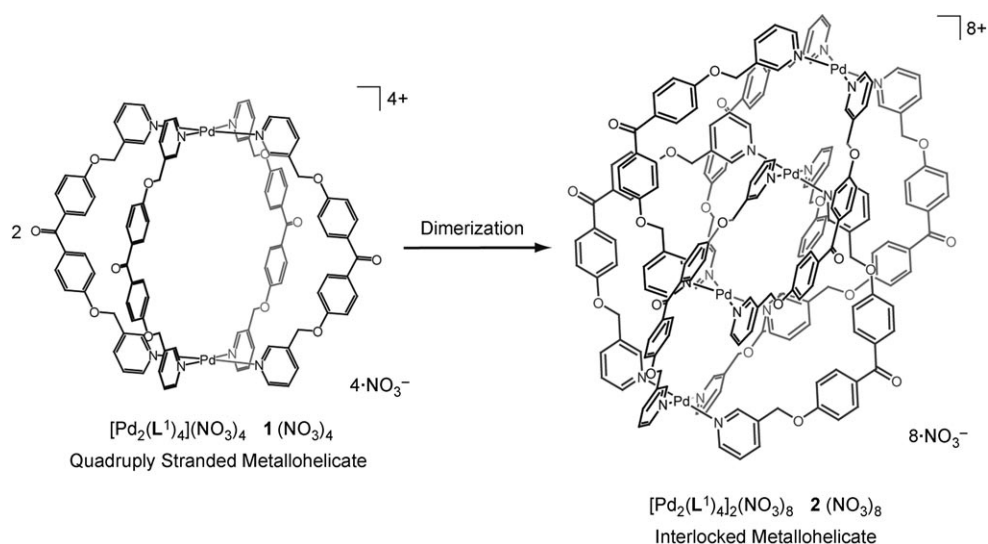


# A Quadruply Stranded Metallohelicate and Its Spontaneous Dimerization into an Interlocked Metallohelicate\*\*

Morihiko Fukuda, Ryo Sekiya,\* and Reiko Kuroda\*

Coordination-driven self-assembly of discrete supramolecular systems ( $[M_xL_y]$  systems;  $M$  = transition-metal ion,  $L$  = ligand) has become one of the most intensely researched fields of current supramolecular chemistry. This is because of its excellent features such as the ease of preparation and high yield of target  $[M_xL_y]$  supramolecules as well as its potential applications in material sciences.<sup>[1]</sup> Over the past two decades, extensive studies have been made on the fabrication of elaborate  $[M_xL_y]$  systems with various morphologies.<sup>[2]</sup> Among them, metallohelicates<sup>[3]</sup> have received particular attention because of their potential use as structural components of functional materials as well as their inherent chirality.<sup>[4]</sup> Although single-, double-, and triple



**Scheme 1.** Schematic illustration of the dimerization of two quadruply stranded metallohelicates (1) to an interlocked metallohelicate (2).

metallohelicates have been well-documented,<sup>[4,5]</sup> quadruply stranded metallohelicates have been rarely reported.<sup>[6]</sup>

Herein we report the design and synthesis of a quadruply stranded metallohelicate and its spontaneous dimerization into an interlocked structure (Scheme 1). Previously, Fujita et al. used rigid ligands and reported an interesting self-assembly of an interlocked supramolecular structure from ten components, as well as the reorganization of two different preformed cages into an interlocked structure by partial decomposition.<sup>[7]</sup> The study described herein shows that a metallohelicate with flexible ligands dimerizes to form an interlocked structure while ultimately keeping the integrity of the monomer unit.

The novelty of our design for the ligand which would give rise to the quadruply stranded metallohelicate lies in the use of benzophenone as the origin of twist: Benzophenone usually adopts a nonplanar  $C_2$  symmetry as a result of steric repulsion between the hydrogen atoms of neighboring phenyl rings and, in solution, the enantiomers are in equilibrium by rapid rotation of the phenyl rings at the  $C_{\text{carbonyl}}-C_{\text{phenyl}}$  bonds. We coupled the benzophenone framework with two flexible 3-pyridylmethoxy groups to create the bridging ligand 4,4'-bis(3-pyridylmethoxy)benzophenone ( $L^1$ ; Scheme 2). Its twisted structure was confirmed by PM6 calculations<sup>[8]</sup> (see Figure S1 in the Supporting Information), which show a dihedral angle of 59.6° between the two phenyl rings of the benzophenone moiety. We expected that self-assembly of  $L^1$  and Pd<sup>II</sup> ions, which prefer to adopt a square-planar geometry,

[\*] Prof. R. Sekiya, Prof. R. Kuroda  
Department of Life Sciences  
Graduate School of Arts and Sciences  
The University of Tokyo  
3-8-1 Komaba, Meguro-ku, Tokyo 153-8902 (Japan)  
Fax: (+81) 3-5454-6601 (for R.S.)  
Fax: (+81) 3-5454-6600 (for R.K.)  
E-mail: csekiya@mail.ecc.u-tokyo.ac.jp  
kuroda@mail.ecc.u-tokyo.ac.jp

M. Fukuda, Prof. R. Kuroda  
Department of Biophysics and Biochemistry  
Graduate School of Science  
The University of Tokyo  
7-3-1 Hongo, Bunkyo-ku, Tokyo 113-0033 (Japan)

Prof. R. Kuroda  
Japan Science and Technology Agency  
ERATO-SORST  
Kuroda Chiro-morphology Team  
4-7-6 Komaba, Meguro-ku, Tokyo 153-0041 (Japan)

[\*\*] We are grateful to the single-crystal X-ray structure analysis group of the RIGAKU corp. for measurement of the diffraction data of **2**. This work was partly supported by a Grant-in-Aid for Scientific Research (17750122) from the Ministry of Education, Culture, Sports, and Technology of Japan.

Supporting information for this article is available on the WWW under <http://www.angewandte.org> or from the author.

would give the target quadruply stranded metallohelicate  $[\text{Pd}_2(\text{L}^1)_4]$  (**1**).

The ligand  $\text{L}^1$  was synthesized in 88 % yield from 3-(chloromethyl)pyridine hydrochloride and 4,4'-dihydroxybenzophenone.<sup>[9]</sup> Colorless crystals of X-ray quality were obtained by slow evaporation of a mixed solvent solution of  $\text{CH}_2\text{Cl}_2$  and hexane at room temperature. Crystallographic analysis<sup>[10]</sup> showed  $\text{L}^1$  to have  $C_2$  symmetry with a dihedral angle of  $49.8^\circ$  (Figure 1). The  $^1\text{H}$  NMR spectrum of  $\text{L}^1$  ( $[\text{D}_6]\text{DMSO}$ ) showed a sharp singlet at  $\delta = 5.20$  ppm corresponding to the methylene protons (Figure 2a), thus indicating a rapid interconversion of the enantiomers on the NMR time scale.

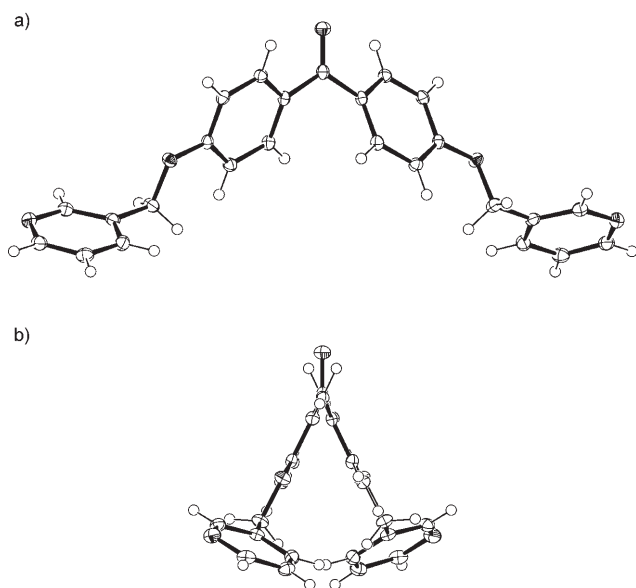


**Figure 1.** ORTEP drawing of 4,4'-bis(3-pyridinemethoxy)benzophenone ( $\text{L}^1$ ; 50 % probability ellipsoid). Top: front view; bottom: side view. Nitrogen and oxygen atoms are represented as shaded ellipsoids.

The reaction of  $\text{L}^1$  with  $\text{Pd}(\text{NO}_3)_2$  (2:1 ratio) in  $[\text{D}_6]\text{DMSO}$  for one hour at room temperature yielded a clear light brown solution (Scheme 2).<sup>[9]</sup> The ESI mass spectrum (see Figure S2 in the Supporting Information) showed a family of prominent signals at  $m/z$  619.9, 960.9, and 1984.9, which were assigned to  $[\text{1}(\text{NO}_3)]^{3+}$ ,  $[\text{1}(\text{NO}_3)_2]^{2+}$ , and  $[\text{1}(\text{NO}_3)_3]^+$ , respectively. These signals indicate the formation of the target metallohelicate. The  $^1\text{H}$  NMR spectrum of the solution showed the quantitative formation of **1**: The pyridyl protons, in particular  $\text{H}_a$  and  $\text{H}_d$ , showed large downfield shifts, a characteristic of metal–ligand complexation (Figure 2a,b, and Table S1 in the Supporting Information). The other pyridyl protons displayed much smaller changes in their chemical shifts. Several attempts to crystallize **1** were unsuccessful.<sup>[11]</sup> A 2D NOESY spectrum (see Figure S3 in the Supporting Information) was thus recorded to elucidate the structure. The NOE signals between the methylene protons ( $\text{H}_e$ ) and the  $\alpha$ - and  $\gamma$ -pyridyl protons ( $\text{H}_a$  and  $\text{H}_b$ ) indicate that the pyridyl rings and the methylene groups are nearly parallel, as observed in the crystal structure

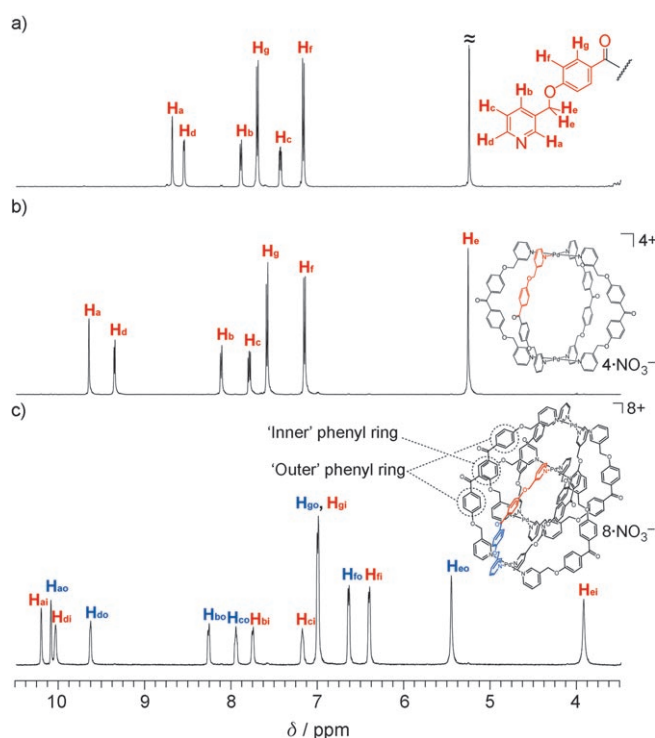
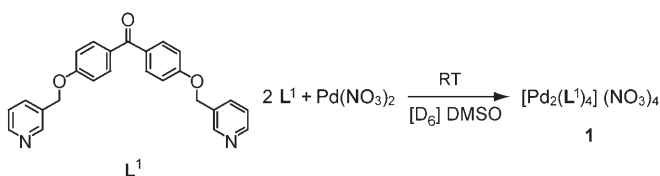


**Figure 2.**  $^1\text{H}$  NMR spectra (500 MHz, 293 K,  $[\text{D}_6]\text{DMSO}$ ) of a) 4,4'-bis(3-pyridinemethoxy)benzophenone ( $\text{L}^1$ ), b)  $[\text{Pd}_2(\text{L}^1)_4](\text{NO}_3)_4$  (**1**), and c)  $[\text{Pd}_2(\text{L}^1)_4]_2(\text{NO}_3)_8$  (**2**). The symmetrically independent parts of  $\text{L}^1$  and **1** are colored red. Those of **2** are colored red or blue.



**Scheme 2.**

of  $\text{L}^1$ . An NOE signal was also observed between  $\text{H}_a$  and  $\text{H}_f$ , but not between  $\text{H}_b$  and  $\text{H}_f$ . This finding indicates that  $\text{H}_a$  points into the inner cage of **1** and is proximal to  $\text{H}_f$  of the ligand as well as to  $\text{H}_f$  of the three neighboring bridging ligands, whereas  $\text{H}_b$  points outward. These structural features are consistent with those of energy-minimized structures of **1** calculated with the universal force-field method (Figure 3).<sup>[12]</sup> The two lowest energy structures have  $D_4$  symmetry, with azimuthal angles  $\theta$  relating the two  $\{\text{PdN}_4\}$  units of  $67.5^\circ$  and  $43.4^\circ$ . In fact, the simple  $^1\text{H}$  NMR spectrum suggests **1** has an even higher symmetry in solution. However, a variable-temperature NMR spectrum of **1** in  $[\text{D}_6]\text{DMSO}/[\text{D}_4]\text{MeOD}$  (1:1)<sup>[13]</sup> showed a broadening of the signal corresponding to  $\text{H}_e$  upon cooling (see Figure S4 in the Supporting Information). Thus, one possible explanation of the higher symmetry is rapid dynamic averaging on the NMR time scale of various conformers, including the energy-minimized structures, in solution, although the possibility of  $C_{4v}$  or  $D_{4h}$  symmetry cannot be excluded entirely.<sup>[14]</sup>

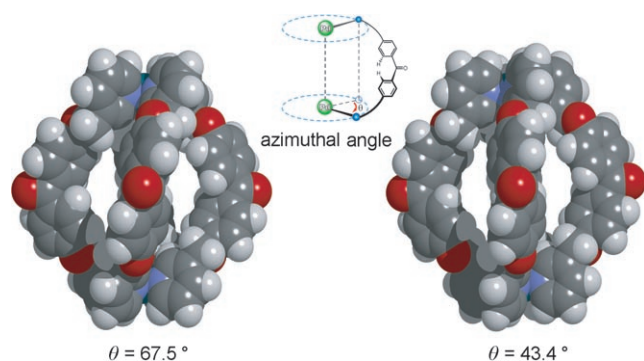


**Figure 3.** The two lowest energy minimized structures of **1** calculated with molecular mechanics calculation using universal force field method (only (M)-twisted **1** is shown).<sup>[14]</sup> Color scheme: gray, carbon; white, hydrogen; blue, nitrogen; red, oxygen; dark green, palladium. Inset: the definition of the azimuthal angle  $\theta$ .

Interestingly, complex **1** was gradually converted into a new complex (**2**) in solution at room temperature, and the rate of the conversion was accelerated on increasing the temperature. To identify the new complex, a freshly prepared solution of **1** in  $[D_6]$ DMSO was heated at 353 K for about 24 h.<sup>[9]</sup> The  $^1\text{H}$  NMR spectrum of the resultant solution (Figure 2c) showed a family of new signals, but no signals for **1**. Further heating of the solution at 353 K resulted in no further change in the NMR spectrum, thus indicating **1** is a kinetic product and **2** is a thermodynamically stable one. It is noteworthy that no signals of intermediates were detected by NMR spectroscopy during the conversion. The ESI mass spectrum (see Figure S5 in the Supporting Information) showed a family of new prominent signals at  $m/z$  620.0, 756.3, 961.6, 1301.9, and 1985.3, which were assigned as  $[\text{Pd}_4(\text{L}^1)_8(\text{NO}_3)_2]^{6+}$ ,  $[\text{Pd}_4(\text{L}^1)_8(\text{NO}_3)_3]^{5+}$ ,  $[\text{Pd}_4(\text{L}^1)_8(\text{NO}_3)_4]^{4+}$ ,  $[\text{Pd}_4(\text{L}^1)_8(\text{NO}_3)_5]^{3+}$ , and  $[\text{Pd}_4(\text{L}^1)_8(\text{NO}_3)_6]^{2+}$ , respectively. This finding suggests that **2** is a dimerized complex of **1**.

X-ray quality single crystals of **2** were obtained by slow diffusion of ethyl acetate vapor into a solution of **2** in DMF at room temperature. Remarkably, crystallographic analysis revealed that **2** is an interlocked metallohelicate composed of two  $\{\text{Pd}_2(\text{L}^1)_4\}$  units (Figure 4).<sup>[15]</sup> This structure is, to the best of our knowledge, the first example of such a structure. Complex **2** resides on a  $C_4$  symmetry axis, with the four  $\text{Pd}^{\text{II}}$  atoms located on it. Interestingly, the two  $\{\text{Pd}_2(\text{L}^1)_4\}$  units in a given molecule of **2** twist in the same direction. The azimuthal angles  $\theta$  of the  $\{\text{Pd}_2(\text{L}^1)_4\}$  units are 21.8 and 8.9° (or their negative values), which are smaller than those of the energy-minimized structures of **1**. This arrangement is mainly due to the compact structure of **2**: CH/ $\pi$  and  $\pi/\pi$  interactions between the neighboring bridging ligands were indicated by the interatomic distances (representative CH/ $\pi$  interactions are shown in Figure S7 in the Supporting Information). Complex **2** has three cages in which nitrate or solvent molecules may be incorporated.<sup>[16]</sup> As the space group is centrosymmetric  $P4/n$ , mirror-image molecules with opposite twist are present in the crystal. No strong intermolecular interactions were found between different complexes of **2**, and DMF molecules were present in the intermolecular space. These observations suggest that the stereochemistry of the

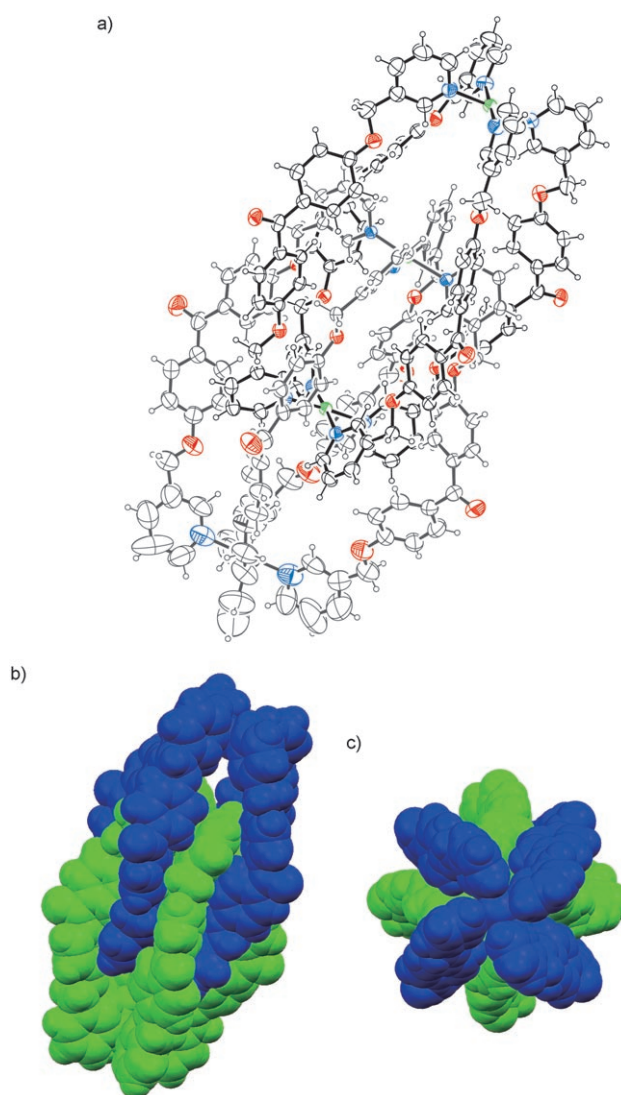


**Figure 4.** a) ORTEP drawing of the X-ray crystal structure of the interlocked metallohelicate **2** (30% probability ellipsoid). Color scheme: gray, carbon; blue, nitrogen; red, oxygen; green, palladium. b) Side view and c) top view of the space-filling illustrations of the X-ray crystal structure of **2**, with one color for each dimer.

complex is not dictated by the crystal packing force (see Figure S6 in the Supporting Information).

Complex **2** retains its interlocked structure in solution. Figure 2b and c show that each signal of the bridging ligands splits into two signals, which suggests that the left and right halves of the bridging ligands experience magnetically different environments. This proposal is supported by the  $^{13}\text{C}$  NMR spectrum, in which all  $^{13}\text{C}$  signals except for that of the carbonyl carbon atom (singlet at  $\delta = 192.2$  ppm) are split into two signals (see Figure S8 in the Supporting Information). The proton signals were fully assigned on the basis of H-H COSY (see Figure S9 in the Supporting Information) and NOESY (see Figure S10 in the Supporting Information) spectra. The protons of the benzophenone framework ( $\text{H}_{\text{co}}$ ,  $\text{H}_{\text{fo}}$ ,  $\text{H}_{\text{ci}}$ , and  $\text{H}_{\text{fi}}$ ) and a 3-pyridinemethoxy arm ( $\text{H}_{\text{bi}}$ ,  $\text{H}_{\text{ci}}$ , and  $\text{H}_{\text{ci}}$ ), except the  $\alpha$ -pyridyl protons ( $\text{H}_{\text{ai}}$  and  $\text{H}_{\text{di}}$ ), experience upfield shifts (see Table S3 in the Supporting Information).



Among them, the upfield shift of  $H_{ei}$  is the largest ( $\Delta_{ppm} = -1.35$  ppm). These shifts are explained by the shielding effect of the neighboring bridging ligands. The large upfield shift of  $H_{ei}$  was expected from the X-ray structure of **2**, in which the methylene protons lie just above the phenyl rings of the benzophenone moieties (see Figure S7 in the Supporting Information). The NOESY spectrum provided important evidence for the interlocked structure (see Figure S10 in the Supporting Information). Of particular interest are the interactions between the  $\beta$ - or  $\gamma$ -pyridyl protons ( $H_{ci}$  or  $H_{bi}$ ) and the benzophenone protons. Normally no NOE signals are observed because of the long distance between them, as found in **1** (see Figure S3 in the Supporting Information). This evidence shows that **2** retains its interlocked structure in solution.

Despite the  $C_4$  symmetry of **2** in the solid state, its  $^1H$  NMR spectrum is simple, which suggests apparent higher symmetry in solution. Variable-temperature NMR measurements of **2** in  $[D_6]DMSO/[D_4]MeOD$  (1:1) showed that, upon cooling the solution, the signals for the protons of the benzophenone frameworks and the methoxy units, especially  $H_{ei}$ ,  $H_{fi}$ , and  $H_{gi}$ , broadened quite significantly compared to those of the pyridyl protons (Figure 5). This result indicates

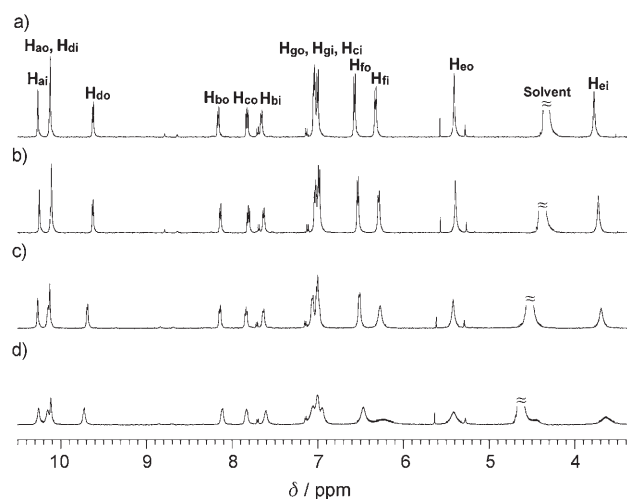


**Figure 5.** Variable-temperature NMR spectra (500 MHz,  $[D_6]DMSO/[D_4]MeOD$  (1:1)) of **2** at a) 273 K, b) 263 K, c) 243 K, and d) 223 K.

that rotation of the phenyl rings becomes slow on the NMR time scale. The signals for  $H_{fi}$  and  $H_{gi}$  ("inner" phenyl rings, see Figure 2c) were much broader than those of  $H_{fo}$  and  $H_{go}$  ("outer" phenyl rings, see Figure 2c) at 223 K. This effect is due to the steric crowding in the central region of **2**. These low-temperature NMR measurements indicate that in solution **2** is in rapid interconversion between various conformers, including the enantiomeric pairs of  $C_4$  symmetry found in the crystal structure.

We further investigated the thermal stability of **2**. Single crystals of **2** were dissolved in  $[D_6]DMSO$  and then the solutions were heated at various temperatures. Below 353 K, **2** was stable, without decomposition. After heating the solutions at 363, 373, and 383 K for several hours, the

$^1H$  NMR spectra of the solutions, which were rapidly cooled to room temperature for measurement of the spectra, showed families of signals of  $L^1$  and **1** as well as of **2** (see Figure S11a in the Supporting Information). Very small amounts of a black precipitate, most likely Pd metal, were formed in the NMR sample tubes. This result means that **2** is highly thermodynamically stable and decomposes slowly to **1** and/or  $L^1$  only at high temperature ( $> 363$  K). After seven days at room temperature, the decomposed **1** was almost completely converted back into **2** (see Figure S11b in the Supporting Information). The remarkable stability of **2** may be ascribed to its compact structure arising from  $CH/\pi$ ,  $\pi/\pi$ , and van der Waals contacts between the neighboring bridging ligands, as found in the crystal structure.

In summary, we have designed and synthesized a new quadruply stranded metallohelicate  $[Pd_2(L^1)_4]$  (**1**), which is formed quantitatively through self-assembly of  $Pd(NO_3)_2$  and the bridging ligand of 4,4'-bis(3-pyridinemethoxy)benzophenone ( $L^1$ ). Complex **1** undergoes spontaneous dimerization into the unprecedented interlocked metallohelicate  $[Pd_2(L^1)_4]_2$  (**2**). We are currently investigating the possibility of dynamic interconversion of chirality as well as the ability of **1** and **2** to encapsulate anions.

Received: July 14, 2007

**Keywords:** cage compounds · helical structures · interlocked structures · self-assembly · supramolecular chemistry

- [1] a) M. Fujita, M. Tominaga, A. Hori, B. Therrien, *Acc. Chem. Res.* **2005**, *38*, 369–378; b) M. Ruben, J. Rojo, F. J. Romero-Salguero, L. H. Uppadine, J.-M. Lehn, *Angew. Chem.* **2004**, *116*, 3728–3747; *Angew. Chem. Int. Ed.* **2004**, *43*, 3644–3662.
- [2] a) G. F. Swiegers, T. J. Malefetse, *Coord. Chem. Rev.* **2002**, *225*, 91–121; b) M. Tominaga, K. Suzuki, M. Kawano, T. Kusukawa, T. Ozeki, S. Sakamoto, K. Yamaguchi, M. Fujita, *Angew. Chem.* **2004**, *116*, 5739–5743; *Angew. Chem. Int. Ed.* **2004**, *43*, 5621–5625.
- [3] J.-M. Lehn, A. Rigault, J. Siegel, J. Harrowfield, B. Chevrier, D. Moras, *Proc. Natl. Acad. Sci. USA* **1987**, *84*, 2565–2569.
- [4] a) C. Piguet, G. Bernardinelli, G. Hopfgartner, *Chem. Rev.* **1997**, *97*, 2005–2062; b) A. E. Rowan, R. J. M. Nolte, *Angew. Chem.* **1998**, *110*, 65–71; *Angew. Chem. Int. Ed.* **1998**, *37*, 63–68.
- [5] a) J. Gregoliński, J. Lisowski, *Angew. Chem.* **2006**, *118*, 6268–6272; *Angew. Chem. Int. Ed.* **2006**, *45*, 6122–6126; b) S. G. Telfer, R. Kuroda, J. Lefebvre, D. B. Leznoff, *Inorg. Chem.* **2006**, *45*, 4592–4601; c) S. G. Telfer, R. Kuroda, *Chem. Eur. J.* **2005**, *11*, 57–68; d) S. G. Telfer, T. Sato, R. Kuroda, *Angew. Chem.* **2004**, *116*, 591–594; *Angew. Chem. Int. Ed.* **2004**, *43*, 581–584; e) J. Hamacek, S. Blanc, M. Elhabiri, E. Leize, A. V. Dorsselaer, C. Piguet, A. M. Albrecht-Gary, *J. Am. Chem. Soc.* **2003**, *125*, 1541–1550; f) R. C. Scarrow, D. L. White, K. N. Raymond, *J. Am. Chem. Soc.* **1985**, *107*, 6540–6546.
- [6] a) D. A. McMorran, P. J. Steel, *Angew. Chem.* **1998**, *110*, 3495–3497; *Angew. Chem. Int. Ed.* **1998**, *37*, 3295–3297; b) L. J. Barbour, G. W. Orr, J. L. Atwood, *Nature* **1998**, *393*, 671–673; c) H. Amouri, L. Mimassi, M. N. Rager, B. E. Mann, C. Guyard-Duhayon, L. Raehm, *Angew. Chem.* **2005**, *117*, 4619–4622; *Angew. Chem. Int. Ed.* **2005**, *44*, 4543–4546; d) J. Xu, K. N. Raymond, *Angew. Chem.* **2006**, *118*, 6630–6635; *Angew. Chem. Int. Ed.* **2006**, *45*, 6480–6485.

- [7] M. Fujita, N. Fujita, K. Ogura, K. Yamaguchi, *Nature* **1999**, *400*, 52–55.
- [8] J. J. P. Stewart, *MOPAC 2007*, <http://openmopac.net/>.
- [9] See the Supporting Information for details.
- [10] Crystal data for **L**<sup>1</sup> ( $C_{25}H_{20}N_2O_3$ ):  $M_r = 198.2$ , colorless crystal, crystal dimensions  $0.40 \times 0.40 \times 0.25 \text{ mm}^3$ , orthorhombic, space group *Pbcn* (no. 60),  $Z = 8$ ,  $\rho_{\text{calcd}} = 1.39 \text{ g cm}^{-3}$ ,  $F(000) = 831.9$ ,  $2\theta_{\text{max}} = 55.8^\circ$  were  $a = 7.1974(5)$ ,  $b = 6.4495(5)$ ,  $c = 40.935(3) \text{ \AA}$ , and  $V = 1900.16(2) \text{ \AA}^3$ . The intensity data were collected on a Bruker SMART APEX CCD diffractometer ( $\text{MoK}\alpha$  radiation,  $\lambda = 0.71073 \text{ \AA}$ ) at 103 K. A total of 10678 reflections were collected of which 2243 reflections were independent ( $R_{\text{int}} = 0.0254$ ). The crystal structure was solved by direct methods using the SHELXS-97 program<sup>[18]</sup> and refined by successive differential Fourier syntheses and full-matrix least-squares procedures using the SHELXL-97 program.<sup>[19]</sup> Anisotropic thermal factors were applied to all non-hydrogen atoms. All hydrogen atoms were generated geometrically. The structure was refined to final  $R_1 = 0.047$  for 2032 data [ $I > 2\sigma(I)$ ] with 137 parameters,  $wR_2 = 0.113$  for all data, GOF = 1.088, and residual electron density max/min =  $0.357/-0.264 \text{ e \AA}^{-3}$ .
- [11] Crystallization of **1** from DMF or DMSO solutions gave only crystals of **2**. We have reasoned that during crystallization, **1** was gradually converted into the thermodynamically more stable **2**. See text for details.
- [12] A. K. Rappe, K. S. Colwell, C. J. Casewit, *Inorg. Chem.* **1993**, *32*, 3438–3450.
- [13] As  $[\text{D}_6]\text{DMSO}$  freezes at 291 K, we used  $[\text{D}_6]\text{DMSO}/[\text{D}_4]\text{MeOD}$  (1:1) mixed solutions for the measurement of the variable-temperature NMR spectra of **1** and **2**. Splitting of the  $\text{H}_c$  signal of **1** was not observed at the lowest possible temperature for the solvent.
- [14] The possibility of **L**<sup>1</sup> having  $C_{2v}$  symmetry with a planar conformation in the complexes and a box shape for **1** was pointed out by one of the referees. PM6 calculations suggested that benzophenone with a planar conformation has a higher heat of formation than the other conformations because of the steric repulsion between hydrogen atoms of neighboring phenyl rings.
- [15] Crystal data for **2** ( $\text{Pd}(\text{C}_{25}\text{H}_{20}\text{N}_2\text{O}_3)_2(\text{DMF})$ ):  $M_r = 972.4$ , colorless crystal, crystal dimensions  $0.11 \times 0.10 \times 0.04 \text{ mm}^3$ , tetragonal, space group *P4/n* (no. 85),  $Z = 8$ ,  $\rho_{\text{calcd}} = 0.90 \text{ g cm}^{-3}$ ,  $F(000) = 4015.4$ ,  $2\theta_{\text{max}} = 54.4^\circ$  were  $a = 20.8580(8)$ ,  $b = 20.8580(8)$ ,  $c = 33.150(2) \text{ \AA}$ , and  $V = 14421.1(1) \text{ \AA}^3$ . The intensity data were collected on a Rigaku Saturn-724 CCD diffractometer ( $\text{MoK}\alpha$  radiation,  $\lambda = 0.71073 \text{ \AA}$ ) at 103 K. A total of 145 124 reflections were collected of which 16 491 reflections were independent ( $R_{\text{int}} = 0.0791$ ). The crystal structure was solved by direct methods using the SIR-2004 program<sup>[20]</sup> and refined by successive differential Fourier syntheses and full-matrix least-squares procedures using the SHELXL-97 program.<sup>[19]</sup> Anisotropic thermal factors were applied to all non-hydrogen atoms. All hydrogen atoms were generated geometrically. The structure was refined to final  $R_1 = 0.124$  for 11 715 data [ $I > 2\sigma(I)$ ] with 592 parameters,  $wR_2 = 0.388$  for all data, GOF = 1.391, and residual electron density max/min =  $1.485/-1.636 \text{ e \AA}^{-3}$ . The diffuse electron density arising from the disordered and unidentified moieties was treated with the SQUEEZE routine within the PLATON software package.<sup>[17]</sup> The final  $\rho_{\text{calcd}}$ ,  $F(000)$ , and  $M_r$  values reflect known contents only. Statistical prior to treatment of data with SQUEEZE were  $R_1 = 0.203$  [ $I > 2\sigma(I)$ ],  $wR_2 = 0.538$  for all data, and GOF = 2.111. CCDC 652008 (**L**<sup>1</sup>) and 652007 contain the supplementary crystallographic data for this paper. These data can be obtained free of charge from The Cambridge Crystallographic Data Centre via [www.ccdc.cam.ac.uk/data\\_request/cif](http://www.ccdc.cam.ac.uk/data_request/cif).
- [16] The highly disordered state of the incorporated molecules meant that none of them could be located, and hence in the final refinement, the electron density within the cages was treated with the SQUEEZE routine in the PLATON program package.<sup>[17]</sup>
- [17] A. L. Spek, *PLATON*, University of Glasgow, Glasgow (Scotland), **1998**.
- [18] G. M. Sheldrick, *SHELXS-97*: Program for X-ray Crystal Structure Solution, University of Göttingen, Göttingen (Germany), **1997**.
- [19] G. M. Sheldrick, *SHELXL-97*: Program for X-ray Crystal Structure Refinement, University of Göttingen, Göttingen (Germany), **1997**.
- [20] M. C. Burla, R. Calandro, M. Camalli, B. Carrozzini, G. L. Casciaro, L. De Caro, C. Giacovazzo, G. Polidori, R. Spagna, *SIR-2004*: A program for automatic solution and refinement of crystal structures.